Role of covalency in the ground state properties of perovskite ruthenates: A first principle study using local spin density approximations

Kalobaran Maiti

Department of Condensed Matter Physics and Material Sciences,
Tata Institute of Fundamental Research, Homi Bhabha Road, Colaba, Mumbai - 400 005, INDIA
(Dated: February 4, 2008)

We investigate the electronic structure of $SrRuO_3$ and $CaRuO_3$ using full potential linearized augmented plane wave method within the local spin density approximations. The ferromagnetic ground state in $SrRuO_3$ could exactly be described in these calculations and the calculated spin magnetic moment is found to be close to the experimentally observed values. Interestingly, the spin polarized calculations for $CaRuO_3$ exhibit large spin moment as observed in the experiments but the magnetic ground state has higher energy than that in the non-magnetic solution. Various calculations for different structural configurations indicate that Ca-O covalency plays the key role in determining the electronic structure and thereby the magnetic ground state in this system.

arXiv:cond-mat/0605553v1 [cond-mat.str-el] 23 May 2006

I. INTRODUCTION

Investigation of the ground state properties of ruthenates has seen an explosive growth in the recent time due to many interesting properties such as superconductivity,[1] non-Fermi liquid behavior,[2,3] unusual magnetic ground states[2,3,4,5] *etc.* observed in these materials. $SrRuO_3$, a perovskite compound exhibits ferromagnetic long range order below the Curie Temperature of about 160 K with a large magnetic moment (1.4 μ_B) despite highly extended $4d$ character of the valence electrons.[4,5] Various band structure calculations based on different kinds of approximations reveal ferromagnetic ground state in $SrRuO_3$ and the calculated magnetic moments are found to strongly depend on the kind of approximations used in the study.[6,7] Interestingly, $CaRuO_3$, an isostructural compound exhibit similar magnetic moment at high temperatures as that observed in $SrRuO_3$ but the magnetic ground state is controversial. While some studies predicted an antiferromagnetic ordering in $CaRuO_3$,[7,8,9,10] various other studies suggest absence of long-range order down to the lowest temperature studied.[2,3,5,11] These later investigations predict that the behavior in this compound is in the proximity of quantum criticality, which is manifested in the transport measurements exhibiting non-Fermi liquid behavior.[2,3]

Both $SrRuO_3$ and $CaRuO_3$ form in an orthorhombic perovskite structure (ABO_3 - type). The space group for $SrRuO_3$ is conventionally defined as *Pbnm* and that for $CaRuO_3$ is *Pnma*, which are essentially the same structure type with a difference in the definition of axis system.[12,13] The A cation (Sr/Ca) sites help to form the typical building block of this structure. The RuO_6 octahedra in these compounds are connected by corner sharing as shown in Fig. 1. The conduction electrons moves via this RuO_6 network and hence determines various electronic properties. The tilting and buckling of the RuO_6 octahedra as evident in the figure essentially leads to a $GdFeO_3$ type distortion resulting to the orthorhombic structure. While the structure type is same in both the
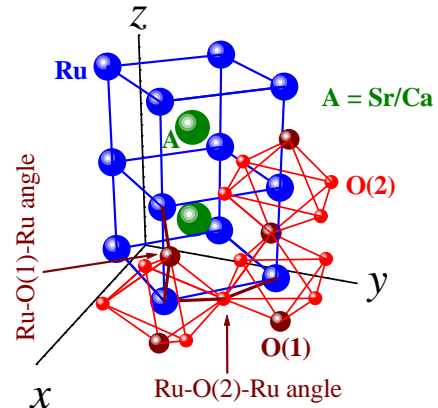

FIG. 1: Schematic diagram of the crystal structure of $SrRuO_3$ and $CaRuO_3$. The thick solid lines show the Ru-O-Ru angles.

compounds, the extent of distortion is somewhat different resulting to a slightly different Ru-O-Ru bond angle in these compounds. If O(1) represents the apical oxygen in the RuO_6 octahedra along z-axis in the figure and O(2) represents the oxygens in the basal (xy) plane, there are two O(2) and one O(1) atoms in one formula unit. The Ru-O-Ru angles in $SrRuO_3$ are:[13] Ru-O(1)-Ru = 167.6°, Ru-O(2)-Ru = 159.7° and those in $CaRuO_3$ are:[14] Ru-O(1)-Ru = 149.6°, Ru-O(2)-Ru = 149.8°.

The Ru-O-Ru angle has significant influence in the electronic properties since the electron hopping interaction strength between Ru-sites via oxygens, usually denoted by t is the largest for the angle of 180° and gradually reduces with the deviation of Ru-O-Ru bond angle from 180°. Thus, the effective electron correlation strength, U/W (U = electron-electron Coulomb repulsion strength and $t \propto W$ = valence band width) is expected to be higher in $CaRuO_3$ than that in $SrRuO_3$. It was believed that the difference in U/W in these two com-

pounds leads to such contrasting ground state properties. However, a recent experimental study shows that U/W is significantly weak as expected for a highly extended $4d$ transition metal oxides and are very similar in *both* the compounds.[15] Thus, the experimental observation of different ground state properties in otherwise these two identical compounds still remains a puzzle despite numerous studies carried out in these and associated other systems as well during last two decades.

Local spin density approximations has often been found to be successful to capture the magnetic ground state properties of various systems.[16,17,18] In the present study, we investigate the magnetic ground state properties of ruthenates using *state-of-the-art* full potential linearized augmented plane wave method[19] within the local spin density approximations. The results for SrRuO$_3$ reveal ferromagnetic ground state consistent with various experimental results. Interestingly, the ground state energy for the spin polarized solution of CaRuO$_3$ is higher than that for the non-magnetic solution despite large exchange splitting leading to a large magnetic moment in this system. Calculations for different structural configurations suggest that Ca-O covalency plays the key role in determining the electronic properties in this system.

II. THEORETICAL METHODS

The electronic band structure calculations were carried out using full potential linearized augmented plane wave (FLAPW) method within the local spin density approximations (LSDA) using WIEN2K software.[19] The lattice constants are obtained from the analysis of x-ray diffraction patterns from high quality polycrystalline samples[4] and are very similar to those estimated earlier for the samples in *both* single crystalline and polycrystalline forms.[12,13,14] The estimated lattice parameters corresponding to the axis system shown in Fig. 1 are; a = 5.572 Å, b = 5.542 Å, c = 7.834 Å for SrRuO$_3$, and a = 5.519 Å, b = 7.665 Å, c = 5.364 Å for CaRuO$_3$. The atomic positions in SrRuO$_3$ used in these calculations are; Sr: $4c$ (x=0.488(3), y=1.00(0), 1/4); Ru: $4b$ (0, 0.5, 0); O(1): $4c$ (x=-0.000(1), y=0.03(8), 1/4); O(2): $8d$ (x=0.28(5), y=0.22(7), z=-0.03(3)). The atomic positions in CaRuO$_3$ are; Ca: $4c$ (x=0.9465(7), 1/4, z=0.0122(5)); Ru: $4b$ (0, 0, 0.5); O(1): $4c$ (x=0.10248(7), 1/4, z=0.5899(1)) and O(2): $8d$ (x=0.2072(5), y=0.4513(5), z=0.2080(8)). It is to note here that the Ru $4d$ orbitals defined in the axis system shown in Fig. 1 are different from those in the local axis system of RuO$_6$ octahedra having t_{2g} and e_g symmetries. In order to show the partial density of states corresponding to different Ru $4d$ orbitals, we have rotated the axis system by 45° in the xy plane and the results are shown later in the text.

Various bond lengths found in these calculations match well with the experimental results. Despite difference in lattice parameters and change in unit cell volume be-
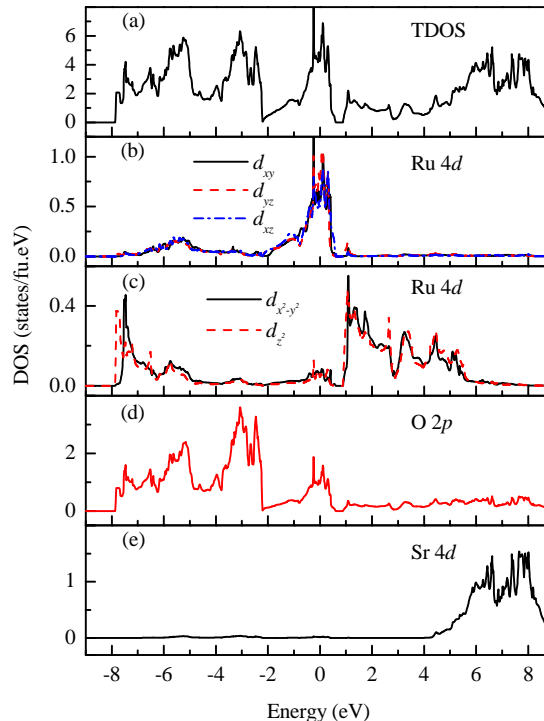

FIG. 2: Calculated (a) TDOS, (b) Ru $4d$ PDOS with t_{2g} symmetry, (c) Ru $4d$ PDOS with e_g symmetry, (d) O $2p$ PDOS, and (e) Sr $4d$ PDOS for the non-magnetic ground state of SrRuO$_3$. The large intensity at the Fermi level suggests a metallic ground state. The states at the Fermi level have primarily Ru $4d$ character with O $2p$ states appearing below - 2 eV.

tween CaRuO$_3$ and SrRuO$_3$, average Ru-O bond lengths are very similar in *both* the cases. The muffin-tin radii (R_{MT}) for Sr/Ca, Ru and O were set to 1.06 Å, 0.85 Å and 0.74 Å, respectively. The convergence for different calculations were achieved considering 512 k points within the first Brillouin zone. The error bar for the energy convergence was set to < 0.25 meV per formula unit. In every case, the charge convergence was achieved to be less than 10^{-3} electronic charge.

III. RESULTS AND DISCUSSIONS

In Fig. 2, we show the density of states (DOS) calculated for the non-magnetic solution of SrRuO$_3$. There are four distinct groups of intense features and a flat region appear in the total density of states (TDOS) shown in Fig. 2(a). In order to identify the character of these features, we also plot the partial density of states (PDOS) corresponding to Ru $4d$, O $2p$ and Sr $4d$ contributions in the eigen states by calculating the projection of the eigen states onto these spin-orbitals. It is clear that Sr $4d$ contributions appear beyond 4 eV above the Fermi level, ϵ_F denoted by 'zero' in the energy axis. O $2p$ also has fi-

nite contributions in this energy range suggesting finite mixing between O $2p$ and Sr $4d$ electronic states.

The Ru $4d$ contributions are shown in two groups. In Fig. 2(b) and 2(c), the $4d$ orbitals defined in the cartesian coordinate systems correspond to the xyz-axis system rotated by $45°$ in the xy plane with respect to the axis system shown in Fig. 1. This axis system is very close to the local axis system of the RuO$_6$ octahedra. The deviations due to the orthorhombic distortions are clearly manifested by small intensities in the energy range corresponding to other symmetries. The d_{xy}, d_{yz} and d_{xz} orbitals possess t_{2g} symmetry and are shown in Fig. 2(b). The PDOS corresponding to these orbitals spread over a large energy range of - 7 eV to 0.6 eV with a sharp feature between - 2 eV to 0.6 eV. O $2p$ PDOS in Fig 2(d) also exhibit significantly large intensities in this energy range. The observation of O $2p$ character in the Ru $4d$ band and vice versa suggests strong hybridization between O $2p$ and Ru $4d$ electronic states. This hybridization between t_{2g} bands and the symmetry adapted O $2p$ bands forms bonding and anti-bonding energy bands, where the overlap of the orbitals are sideways and are known as π-bonds. The energy bands between - 7 eV to - 4.5 eV energies can be assigned as bonding bands and the anti-bonding bands appear between - 2 to 0.6 eV. From the relative intensities of the Ru $4d$ and O $2p$ PDOS, it is evident that the anti-bonding bands possess essentially Ru $4d$ character and the bonding bands have O $2p$ character. The total width of the t_{2g} band is close to 2.6 eV.

The $d_{x^2-y^2}$ and d_{z^2} PDOS are shown in Fig. 2(c). The primary contribution appears between 0.9 eV and 5.5 eV with large contributions between - 7.8 eV to - 5 eV. Similar to the case of t_{2g} bands, significant O $2p$ PDOS also appear in these energy ranges. The mutual contributions between Ru $4d$ and O $2p$ states again indicate large degree of covalency. The electronic states with e_g symmetry form σ-bonds (head-on overlap) with the O $2p$ states. Since, σ-bonds are significantly stronger than the π-bonds, it is expected that the separation between bonding and anti-bonding states involving σ-bonds will be significantly larger compared to that corresponding to π-bonds. This is clearly manifested in the electronic density of states in Fig. 2(c), where the energy region between - 7.8 eV and - 5 eV is contributed by bonding bands with dominant O $2p$ character and the anti-bonding states appear above ϵ_F.

The features in the energy region between - 4 eV to - 2.2 eV are primarily contributed by O $2p$ PDOS, and has negligible contributions from Ru $4d$ and Sr $4d$ electronic states. Thus, these intensities are assigned to the O $2p$ non-bonding electronic states. Notably, all these characterizations are consistent with various photoemission results.[15]

In order to investigate the magnetic properties in this system within the local spin-density approximations, we have calculated the ground state energies for ferromagnetic arrangement of moments of the constituents. Inter-
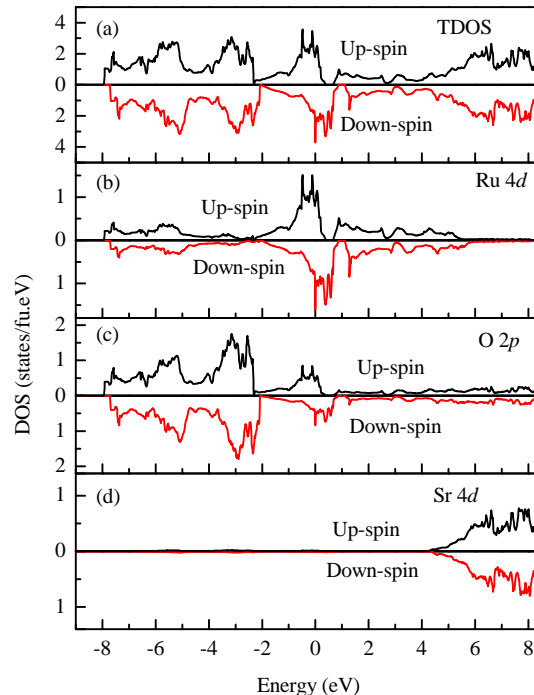

FIG. 3: Calculated (a) TDOS, (b) Ru $4d$ PDOS, (c) O $2p$ PDOS, and (d) Sr $4d$ PDOS for the ferromagnetic ground state of SrRuO$_3$. The down spin DOS are shown in the same energy scale with inverted DOS axis.

estingly, the eigen energy for the ferromagnetic ground state is lower by 1.2 meV per formula unit (fu) than the lowest eigen energy for the non-magnetic solution. It is to note here that a small variation in atomic position leads to a large difference in energy between the ground state energies corresponding to ferromagnetic and non-magnetic solutions. For example, for the atomic positions from Ref. [12], this energy difference is about 9 meV /fu. However, the ferromagnetic ground state energy in this case is 612 meV /fu higher than that in the present case. Interestingly, all the structures of SrRuO$_3$ published in the literature to my knowledge, the ferromagnetic ground state energy is observed to be lower than that corresponding to the non-magnetic solution. While these results are clearly consistent with the experimental observations and various previous results,[6,7] it reestablishes that the local spin density approximations are sufficient to capture the magnetic ground state in these materials as also established in $3d$ and $5d$ transition metal oxides.[16,17,18]

The spin magnetic moment centered at Ru-sites is found to be about 0.58 μ_B, which is substantially small compared to the spin only value of 2 μ_B corresponding to four electrons in the t_{2g} orbitals in the low spin configuration of Ru^{4+}. In addition, there is a large spin polarization of the interstitial electronic states ($\sim$ 0.33 μ_B $\Rightarrow$ about 57% of the Ru-moment). The induced spin moment at the oxygen sites are also found to be significantly large (0.1 μ_B for O(1) and 0.08 μ_B for O(2)). All

these magnetic moments centered at different Ru and O sites couple ferromagnetically. Thus, the total spin magnetic moment per formula unit is found to be about 1.2 μ_B and is very close to the experimental estimation of 1.4 $\pm$ 0.4 μ_B from various measurements on varieties of samples in single and polycrystalline forms.[9,20]

Interestingly, the total magnetic moment, although consistent to the experimental estimations, is significantly lower than the spin only value for the $t_{2g\uparrow}^3 t_{2g\downarrow}^1$ electronic configuration for Ru^{4+} ions. This is significantly different from $3d$ transition metal oxides, where the calculated magnetic moment is often found very close to their spin only value corresponding to the electronic configuration close to the transition metal ions. While it has been observed that various other approximations, such as generalized gradient approximations, inclusion of spin-orbit coupling *etc.* leads to a larger value of the spin magnetic moment in the ground state, the experimental observation of small saturation magnetic moment even for high quality single crystals suggests that other effects are important for this system. In particular, the orbital moment is expected to be negligible for these large $4d$ orbitals due to the strong crystal field effect. The reduction of local moment from the spin only value of 2 μ_B may be attributed to the highly extended nature of the $4d$ orbitals. In addition, a large degree of O $2p$ - Ru $4d$ hybridization is observed in the DOS, which may reduce the magnetic moment further.

The shifts in the DOS due to exchange splitting are shown in Fig. 3, where the down-spin DOS is shown on the same energy scale (x-axis) but the DOS-axis is inverted. The relative shift of the up- and down-spin states provides an estimation of the exchange splitting of the corresponding electronic states. It is evident that there is no shift between up- and down-spin Sr $4d$ states appearing above 4 eV. The relative shift in the up- and down-spin PDOS corresponding to O $2p$ states provides an estimate of the exchange splitting of about 0.25 eV. The exchange splitting in Ru $4d$ total density of states is close to 0.5 eV and is consistent with the values obtained in previous studies.[6] However, it is found to be somewhat different for the electronic states with different symmetries. While it is 0.5 eV for t_{2g} bands, close to 0.4 eV is observed in the case of e_g bands. Smaller splitting in the later cases may be attributed to the larger degree of itinerancy of the corresponding electronic states. Interestingly, the TDOS at ϵ_F for the up-spin states is found to be significantly smaller (1.95 states/eV.fu) than that (3.64 states/eV.fu) for the down spin states. The spin polarization can be defined as

$$P = \frac{(N(\epsilon_F)_\uparrow - N(\epsilon_F)_\downarrow)}{(N(\epsilon_F)_\uparrow + N(\epsilon_F)_\downarrow)}$$

where $N(\epsilon_F)$ denotes the density of state at ϵ_F. Thus, P is found to be - 30.2%, which is significantly large and negative as observed experimentally.[21]

We now turn to the case of $CaRuO_3$. The calculated DOS for non-magnetic solutions are shown in Fig. 4. The
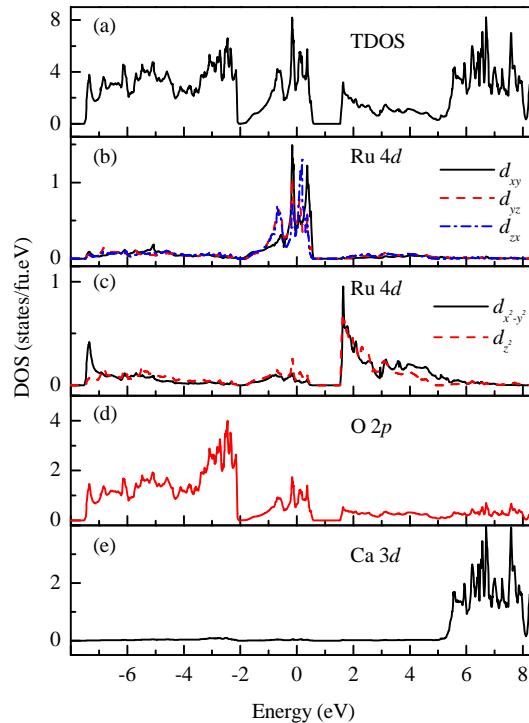

FIG. 4: Calculated (a) TDOS, (b) Ru $4d$ PDOS with t_{2g} symmetry, (c) Ru $4d$ PDOS with e_g symmetry, (d) O $2p$ PDOS, and (e) Ca $3d$ PDOS for the non-magnetic ground state of $CaRuO_3$. The large intensity at the Fermi level suggests a metallic ground state as that observed in $SrRuO_3$. The states at the Fermi level have primarily Ru $4d$ character with O $2p$ states appearing below - 2 eV.

features below - 2 eV is primarily contributed by the O $2p$ PDOS as also observed in the case of $SrRuO_3$ in Fig. 2. The oxygen $2p$ non-bonding bands appear between - 4 eV to - 2 eV energy range. By comparing the Ru $4d$ PDOS and O $2p$ PDOS, it is evident that the bonding t_{2g} and e_g bands with dominant O $2p$ character appears below - 4 eV, where the bonding e_g bands have the lower energies as expected. The anti-bonding t_{2g} bands possess dominant Ru $4d$ character and appear between - 1.8 eV to 0.6 eV energies. The anti-bonding e_g bands appear between the energy range of 1.5 eV to 5 eV. The t_{2g} and e_g bands are separated by a distinct energy gap of about 1 eV. Interestingly, *Ca 3d contributions appear above 5 eV, which is significantly higher than the energy range corresponding to the Sr 4d contributions.* This is unusual since the Sr $4d$ electronic states are expected to have higher energies compared to the energies of Ca $3d$ electronic states. We will discuss this unusual observation later in the text.

It is to note here that the total width of the t_{2g} band is about 2.4 eV, which is slightly smaller than that observed for $SrRuO_3$ ($\sim$ 2.6 eV; a change of 7.5%). However, the width of the individual d-bands are very close to each other ($\sim$ 2.4 $\pm$ 0.1 eV). Thus, the smaller Ru-O-Ru
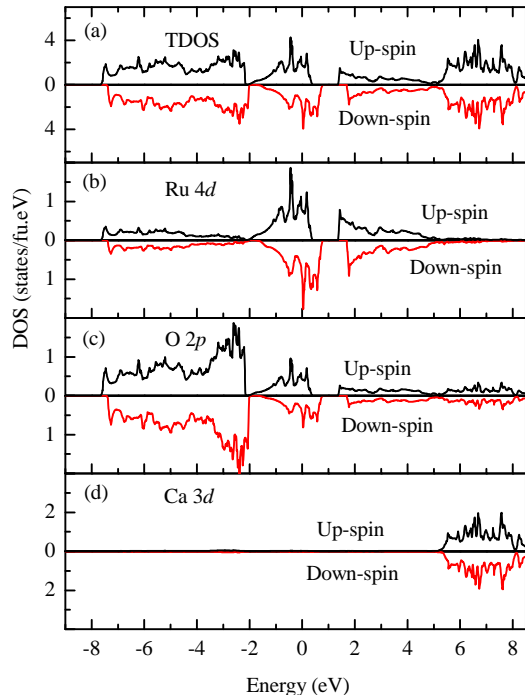
FIG. 5: Calculated (a) TDOS, (b) Ru $4d$ PDOS, (c) O $2p$ PDOS, and (d) Ca $3d$ PDOS for the ferromagnetic ground state of CaRuO$_3$. The down spin DOS are shown in the same energy scale with inverted DOS axis.

bond angle in CaRuO$_3$ has very little influence on the width of the t_{2g} bands. While all the d bands with t_{2g} symmetry are very similar in SrRuO$_3$, the d_{xy} band in CaRuO$_3$ is slightly shifted to higher energies compared to the d_{yz} and d_{xz} bands. This energy shift may be attributed to the distortion of the RuO$_6$ octahedra leading to a deviation from octahedral symmetry towards D_{4h} symmetry. The width of the e_g band is found to be smaller (~ 3.5 eV) in CaRuO$_3$ than that (~ 4.6 eV) in SrRuO$_3$. Since, e_g states are coupled with oxygens via σ bonds, the change in Ru-O-Ru bond angle has the strongest influence in these bands in comparison to that in the π-bonded case corresponding to t_{2g} bands. However, such changes will not have significant influence in the electronic properties of these materials since the e_g bands are essentially empty in both the compounds.

In order to probe the magnetic properties in this system, we calculated the lowest energy eigen states for the ferromagnetic ordering of the spin moments at various sites. Interestingly, the calculations converges to a ferromagnetic ground state with large spin moments at different sites and the lowest energy eigenvalue is slightly (4 meV /fu) higher than that for the non-magnetic solution. A recent study[7] using full potential linearized muffin-tin orbital (FPLMTO) calculations within generalized gradient approximations (GGA) and spin-orbit coupling shows that CaRuO$_3$ exhibit G-type antiferromagnetic long range order, where all the neighboring Ru-sites are antiferromagnetically coupled. However, in the absence of spin-orbit coupling, the ground state is found to be ferromagnetic. There are strong controversy in the ground state behavior in CaRuO$_3$. The recent studies suggest an enhanced paramagnetic ground state[5] and/or proximity to the quantum criticality.[2] Slightly higher energy corresponding to the ferromagnetic ground state compared to the non-magnetic/paramagnetic solutions in this study suggests that ferromagnetic ground state in not stable in this systems as also observed in the experimental results.

In the ferromagnetic solution, the spin magnetic moment centered at the muffin-tin spheres corresponding to Ru, O(1), O(2) and interstitial states are found to be 0.49 μ_B, 0.04 μ_B, 0.08 μ_B and 0.25 μ_B, respectively. All the spin magnetic moments at different sites couple ferromagnetically, which leads to a total spin magnetic moment of about 1 μ_B. This value is again significantly smaller than the spin only value of 2 μ_B for Ru^{4+} but consistent with the experimentally observed values.[4,5] In order to investigate the up- and down spin DOS corresponding to various elements in CaRuO$_3$, we show the calculated DOS in Fig. 5 in the same way as shown in Fig. 3 for SrRuO$_3$. The exchange splitting in O $2p$ PDOS is found to be about 0.25 eV. The exchange splitting in *both* t_{2g} and e_g bands is close to 0.4 eV, which is slightly smaller than that observed in SrRuO$_3$. No exchange splitting is observed for Ca $3d$ states. The TDOS at ϵ_F for the up and down spin states are 1.75 states/eV.fu and 2.22 states/eV.fu, respectively. Thus, the spin polarization at ϵ_F in this compound is found to be about - 11.9%.

From the results presented so far, it is clear that the observation of ferromagnetism in SrRuO$_3$ can be explained by band structure effects. The lowest eigen energies for different magnetic arrangements in CaRuO$_3$ suggest a nonmagnetic/paramagnetic ground state. In order to investigate the origin of such difference in CaRuO$_3$ compared to SrRuO$_3$, we calculated the lowest energy eigen states for different combinations of crystal structures and their magnetic ground states. As a first step, we calculated the lowest energy solutions for SrRuO$_3$ in the same crystal structure as that of CaRuO$_3$. Interestingly, the lowest eigen energy for the nonmagnetic solution is 1117.5 meV /fu higher than the ferromagnetic ground state energy in its real structure. The lowest eigen energy for the ferromagnetic solutions in this crystal structure is even higher (1118.5 meV /fu). The total spin magnetic moment is found to be very very small (0.14 μ_B). Change in structure reduces the unit cell volume by about 6.4% and the average Ru-O-Ru bond angle from 165° to 150°. However, average Ru-O bond lengths are very similar. The large increase in energy indicates that such changes does not lead to a stable state. Interestingly, in the CaRuO$_3$ structure, the ferromagnetic ordering leads to an enhancement in eigen energies compared to the non-magnetic solutions although Sr is present at the A-sites.

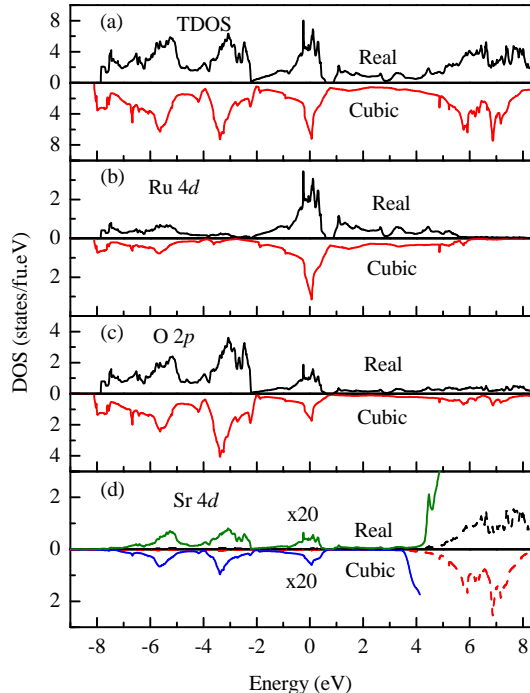We now compare the lowest eigen energies calcu-

FIG. 6: Comparison of (a) TDOS, (b) Ru 4d PDOS, (c) O 2p PDOS and (d) Sr 4d PDOS of SrRuO$_3$ in the real structure (positive DOS axis) and equivalent cubic structure (inverted DOS axis). Results exhibit a close similarity between the two cases as expected in SrRuO$_3$. In (d), the dashed lines represent the calculated DOS and the solid lines represented the same multiplied by 20.

FIG. 7: Comparison of (a) TDOS, (b) Ru 4d PDOS, (c) O 2p PDOS and (d) Ca 3d PDOS of CaRuO$_3$ in the real structure (positive DOS axis) and equivalent cubic structure (inverted DOS axis). A large shift of the Ca 3d band suggests strong Ca-O covalency. In (d), the dashed lines represent the calculated DOS and the solid lines represented the same multiplied by 20.

lated for CaRuO$_3$ in the crystal structures similar to that of SrRuO$_3$. The lowest eigen energy increases by 893.6 meV /fu compared to the ground state energy in its original structure in the nonmagnetic/paramagnetic configuration. Interestingly, the ferromagnetic solution is 869.7 meV /fu higher in energy, which is 23.9 meV /fu lower than that in the nonmagnetic configuration. The magnetic moment calculated in this configuration is 0.66 μ_B, 0.05 μ_B, 0.12 μ_B and 0.39 μ_B for Ru, O(1), O(2) and interstitial states, respectively. The total magnetic moment is found to be 1.35 μ_B, which is significantly higher than that found even in SrRuO$_3$. Thus, in SrRuO$_3$ structure, the presence of Ca at the A-sites also stabilizes ferromagnetic ground state. Since the change in structure is essentially reflected in the Ru-O-Ru bond angle without much change in Ru-O bond length, it is clear that this change in bond-angle helps to stabilize ferromagnetic ground state. *The A-site potential in the ABO$_3$ structure has negligible influence in determining the magnetic ordering of the compound.*

In order to probe the role of cations in stabilizing the crystal structure, which is manifested by large change in the ground state energies, we compare the calculated results for both SrRuO$_3$ and CaRuO$_3$ for their real structure and the equivalent cubic structure keeping the
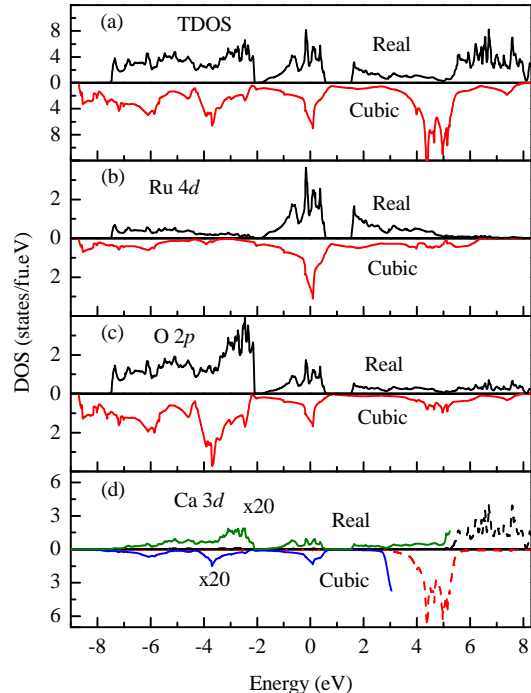
unit cell volume identical to that in the real structure. The ground state energy for the nonmagnetic solution of SrRuO$_3$ is about 45 meV /fu higher than the ferromagnetic ground state energy in the real structure. The calculated DOS are shown in Fig. 6. It is evident that the DOS for real and cubic structures are similar in terms of energy position and overlap of Ru 4d and Sr 4d electronic states with the O 2p states *etc.* Total width of various bands are somewhat narrower in the real structure compared to that in the cubic structure. It is to note here that GdFeO$_3$ type of distortion appears in SrRuO$_3$ via the distortion of the RuO$_6$ octahedra with different Ru-O bond lengths, and Ru-O(1)-Ru bond angle 167.6° and Ru-O(2)-Ru bond angle 159.7°. This leads to a lifting of degeneracy of the t_{2g} and e_g bands. However, the average Ru-O bond lengths are close to that in the equivalent cubic structure. This is clearly manifested by the closeness of the DOS and PDOS shown in Fig. 6.

In CaRuO$_3$, the nonmagnetic ground state energy in the cubic structure is significantly large ($\sim$ 190 meV /fu) compared to that in the real structure. We compare the calculated DOS corresponding to the real structure of CaRuO$_3$ and the equivalent cubic structure in Fig. 7. The width of the Ru 4d and O 2p bands are significantly larger in the cubic structure due to the Ru-O-Ru bond
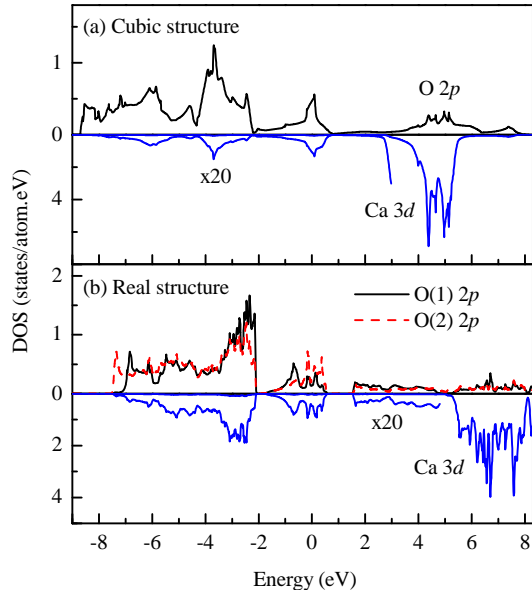
FIG. 8: (a) Ca $3d$ PDOS is compared with O $2p$ PDOS in the cubic structure, where the unit cell volume is identical to the unit cell volume in the real structure. (b) Ca $3d$ PDOS is compared with O(1) $2p$ PDOS and O(2) $2p$ PDOS corresponding to the real structure of $CaRuO_3$. The results suggest a strong Ca-O(1) covalency.

angle of 180° and a smaller Ru-O bond length arising from smaller unit cell volume. The most striking effect is observed in the PDOS of Ca $3d$ band. In the results corresponding to the cubic structure, Ca $3d$ band appear in the energy range of 3 - 5.5 eV as expected for Ca $3d$ electronic states compared to the energies of Sr $4d$ electronic states shown in Fig. 6. Such lower binding energies leads to a significant overlap with the O $2p$ PDOS appearing at lower energies. Interestingly, the Ca $3d$ PDOS contributions shift to above 5 eV energies in the real structure with an increase in contribution in the O $2p$ dominated region as shown by expanding the low energy part in Fig. 7(d).

In order to investigate the Ca-O covalency and the overlap with different oxygens in the structure, we plot Ca $3d$ PDOS along with corresponding O(1) $2p$ and O(2) $2p$ PDOS in Fig. 8. In the cubic structure, Ca $3d$ PDOS appears between 3 eV and 5.5 eV energies. The contributions at lower energies ($E < \epsilon_F$) appears to have different intensity distribution with energy compared to that observed for O $2p$ PDOS. In the real structure, the Ca $3d$ band shifts to above 5 eV energies and the contributions below ϵ_F matches significantly well with the PDOS corresponding to O(1) $2p$ electronic states. This reveals a typical scenario of Ca $3d$ and O(1) $2p$ hybridization resulting to bonding and antibonding bands. The bands at lower energies represent the bonding electronic states with dominant O $2p$ character and the antibonding levels with large Ca $3d$ character shifts to higher energies.

Thus, *the DOS in the real structure reveals a large degree of covalency between Ca-O(1) in the structure, which leads to a shift of O(1) sites towards Ca-sites (GdFeO₃ type of distortion).*[22]

Smaller ionic radius of Ca^{2+} compared to Sr^{2+} leads to a reduction in Goldschmidt tolerance factor ($r_A + r_O)/\sqrt{2}(r_{Ru} + r_O)$, where r_A is the ionic radius of Sr/Ca. Such reduction often results to a distortion in the crystal structure. However, this does not indicate, what kind of distortion is expected. In $3d^1$ perovskite systems, it is already shown that although there is no change in the tolerance factor between $CaVO_3$ and $LaTiO_3$, a large distortion in the crystal structure is observed.[22] It was shown that the covalency between A-site cations and O-$2p$ states plays the key role in determining the distortion in the crystal structure and that the shift of O(1) sites towards A-sites leads to a GdFeO₃-type of distortion in these systems. A similar effect is also observed here in the electronic structure of these perovskite ruthenates.

In order to understand the magnetic ground state in $CaRuO_3$ in the cubic structure, we have calculated the lowest eigen energies for the same unit cell. Interestingly, in the cubic structure, the ground state is ferromagnetic, which is about 21 meV /fu lower in energy than that for non-magnetic solution. The magnetic moment is found to be significantly large with total spin contribution of 1.2 μ_B. The Ru-O bond length in this condition is about 1.92 Å, which is significantly smaller than that in the real structure (average bond length $\cong$ 2 Å). It has been observed that application of pressure leads to a decrease in Curie temperature in $SrRuO_3$.[23] This has also been observed in our calculations as well as in the theoretical results published in the past[6] that ferromagnetic solution becomes less stable with the decrease in unit cell volume leading to a decrease in Ru-O-Ru bond angle. Thus, *the observation of ferromagnetic ground state in the cubic structure of $CaRuO_3$ clearly reveals an important role of Ru-O-Ru bond angle in the ground state properties.*

In $3d$ transition metal (TM) oxides, it is observed that the TM-O-TM superexchange interaction stabilizes antiferromagnetic ordering for TM-O-TM bond angles of 180°. This is the origin of antiferromagnetic behavior observed in almost all the $3d$ transition metal oxides with insulating ground state. For TM-O-TM bond angle of 90°, a ferromagnetic ordering is expected since the oxygen $2p$ orbitals connected to two neighboring TM sites are orthogonal and the holes transferred from TM sites will be parallel due to Hund's rule coupling. Thus, a deviation from 180° is expected to help ferromagnetic ordering due to Hund's rule effect.

In addition, the deviation of Ru-O-Ru bond angle from 180° is expected to enhance the local magnetic moment of $4d$ electronic states due to the decrease in hopping interactions strength. Thus, *the destabilization of the long range ferromagnetic order in $CaRuO_3$ due to the decrease in Ru-O-Ru angle from 180° is unusual.*

It is to note here that in $3d$ transition metal oxides, the magnetic moment at the transition metal site is often

8

found to be very close to the values corresponding to the ionic configuration[16,17] suggesting significantly large localized character of the $3d$ electrons. However, $4d$ orbitals are highly extended compared to the $3d$ orbitals and the correlation effects are found to be significantly weak.[15] This is clearly manifested in various magnetic measurements with the estimations of significantly smaller magnetic moment (close to $1.4\,\mu_B$) compared to the spin-only value of $2\,\mu_B$ for Ru^{4+}. The extended nature of the $4d$ electronic states leads to a strong coupling between the local moments centered at different cites. This is presumably the origin of large degree of spin polarization in the O $2p$ bands ($\geq 17\%$) and in the interstitial electronic states ($\geq 55\%$). Such large spin polarization of the valence electronic states has also been observed in elemental ferromagnets; $4f$ moments leads to a strong spin polarization in the $5d6s$ valence electrons of Gd[24]

and these electronic states couple the local moments at different sites leading to a ferromagnetic long range order. Such coupling is will be weaker in these ruthenates, when the Ru-O-Ru angle deviates from $180°$ due to the reduction in hopping interaction strength and hence the reduction in extended nature of the valence electrons. While these arguments provide a qualitative understanding of the magnetic properties in these interesting class of materials, further study is required to probe the details of such interactions in these systems.

In summary, the results in these calculations establishes that A-O covalency in the $ARuO_3$ structure plays the key role in determining the electronic structure in these systems. The absence of long range order in $CaRuO_3$ may be attributed to smaller Ru-O-Ru angle appearing due to large Ca-O covalency in this system.

[1] Y. Maeno *et al.*, Nature **372**, 532 (1994).
[2] P. Khalifah, I. Ohkubo, H. Christen, and D. Mandrus, Phys. Rev. B **70**, 134426 (2004); Y. S. Lee, Jaejun Yu, J. S. Lee, T. W. Noh, T.-H. Gimm, Han-Yong Choi, and C. B. Eom, Phys. Rev. B **66**, 041104(R) (2002).
[3] L. Klein, L. Antognazza, T.H. Geballe, M.R. Beasley, and A. Kapitulnik, Phys. Rev. B **60**, 1448 (1999).
[4] R.S. Singh, P.L. Paulose, and K. Maiti, Solid State Physics: Proceedings of the DAE Solid State Physics Symposium **49**, 876 (2004).
[5] G. Cao, S. McCall, M. Shepard, J.E. Crow, and R.P. Guertin, Phys. Rev. B **56**, 321 (1997).
[6] David J. Singh, J. Appl. Phys. **79**, 4818 (1996).
[7] R. Vidya, P. Ravindran, A. Kjekshus, H. Fjellvag, and B.C. Hauback, J. Solid State Chem. **177**, 146 (2004).
[8] A. Callaghan, C.W. Moeller, and R. Ward, Inorg. Chem. **5**, 1572 (1966).
[9] J.M. Longo, P.M. Raccah, and J.B. Goodenough, J. Appl. Phys. bf 39, 1327 (1968).
[10] T. Sugiyama and N. Tsuda, J. Phys. Soc. Jpn. **68**, 3980 (1999).
[11] J.L. Martinez, C. Prieto, J. Rodriguez-Carvajal, A. de Andrés, M. Valet-Regi, and J.M. Gonzaler-Calbet, J. Magn. Magn. Mater. **140-144**, 179 (1995).
[12] M.V. Rama Rao, V.G. Sathe, D. Sornadurai, B. Panigrahi, and T. Shripathi, J. Phys. Chem. Solids **62**, 797 (2001).
[13] H. Nakatsugawa, E. Iguchi, and Y. Oohara, J. Phys.: Condens. Mater **14**, 415 (2002).
[14] H. Kobayashi, M. Nagata, R. Kanno, and Y. Kawamoto, Mater. Res. Bull. **29**, 1271 (1994).
[15] K. Maiti and R.S. Singh, Phys. Rev. B **71**, 161102(R) (2005).
[16] D. D. Sarma, N. Shanthi, S. R. Barman, N. Hamada, H. Sawada, and K. Terakura, Phys. Rev. Lett. **75**, 1126 (1995).
[17] N. Hamada, H. Sawada, I. Solovyev, and K. Terakura, Physica B **237-238**, 11 (1997).
[18] K. Maiti, Phys. Rev. B **73**, 115119 (2006).
[19] P. Blaha, K. Schwarz, G.K.H. Madsen, D. Kvasnicka, and J. Luitz, **WIEN2k**, An Augmented Plane Wave + Local Orbitals Program for Calculating Crystal Properties (Karlheinz Schwarz, Techn. Universität Wien, Austria), 2001. ISBN 3-9501031-1-2.
[20] A. Kanbayashi, J. Phys. Soc. Jpn. **44**, 108 (1978).
[21] D.C. Worledge and T.H. Geballe, Phys. Rev. Lett. **85**, 5182 (2000).
[22] E. Pavarini, S. Biermann, A. Poteryaev, A. I. Lichtenstein, A. Georges, and O. K. Andersen, Phys. Rev. Lett. **92**, 176403 (2004); E. Pavarini, A. Yamasaki, J. Nuss, and O.K. Andersen, cond-mat/0504034.
[23] J.J. Neumeier, A.L. Cornelius, and J.S. Schiling, Physica B **198**, 324 (1994).
[24] K. Maiti, M.C. Malagoli, A. Dallmeyer, and C. Carbone, Phys. Rev. Lett. **88**, 167205 (2002).